ACCOUNTS
of chemical research

Surface Chemistry for Molecular Layer Deposition of Organic and Hybrid Organic–Inorganic Polymers

STEVEN M. GEORGE,*,†,‡ BYUNGHOON YOON,† AND ARRELAINE A. DAMERON†,§

†Departments of Chemistry and Biochemistry, and ‡Chemical and Biological Engineering, University of Colorado, Boulder, Colorado 80309

RECEIVED ON APRIL 13, 2008

CONSPECTUS

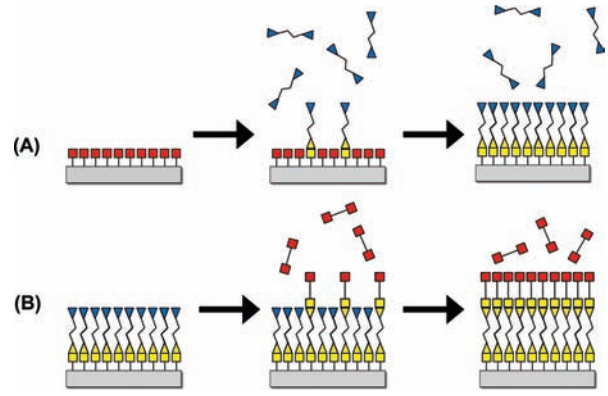

The fabrication of many devices in modern technology requires techniques for growing thin films. As devices miniaturize, manufacturers will need to control thin film growth at the atomic level. Because many devices have challenging morphologies, thin films must be able to coat conformally on structures with high aspect ratios. Techniques based on atomic layer deposition (ALD), a special type of chemical vapor deposition, allow for the growth of ultra-thin and conformal films of inorganic materials using sequential, self-limiting reactions. Molecular layer deposition (MLD) methods extend this strategy to include organic and hybrid organic–inorganic polymeric materials.

In this Account, we provide an overview of the surface chemistry for the MLD of organic and hybrid organic–inorganic polymers and examine a variety of surface chemistry strategies for growing polymer thin films. Previously, surface chemistry for the MLD of organic polymers such as polyamides and polyimides has used two-step AB reaction cycles using homo-bifunctional reactants. However, these reagents can react twice and eliminate active sites on the growing polymer surface. To avoid this problem, we can employ alternative precursors for MLD based on hetero-bifunctional reactants and ring-opening reactions. We can also use surface activation or protected chemical functional groups.

In addition, we can combine the reactants for ALD and MLD to grow hybrid organic–inorganic polymers that should display interesting properties. For example, using trimethylaluminum (TMA) and various diols as reactants, we can achieve the MLD of alucone organic–inorganic polymers. We can alter the chemical and physical properties of these organic–inorganic polymers by varying the organic constituent in the diol or blending the alucone MLD films with purely inorganic ALD films to build a nanocomposite or nanolaminate. The combination of ALD and MLD reactants enlarges the number of possible sequential self-limiting surface reactions for film growth. Extensions to three-step ABC reaction cycles also offer many advantages to avoid the use of homo-bifunctional reactants and incorporate new functionality in the thin film.

The advances in ALD have helped technological development in many areas, including semiconductor processing and magnetic disk-drive manufacturing. We expect that the advances in MLD will lead to innovations in polymeric thin-film products. Although there are remaining challenges, effective surface chemistry strategies are being developed for MLD that offer the opportunity for future advances in materials and device fabrication.

1. Introduction

Atomic layer deposition (ALD) is a special type of chemical vapor deposition (CVD) that is based on two sequential, self-limiting surface reactions.[1,2] Because the surface reactions are self-limiting, ALD can deposit conformal ultra-thin films on high aspect ratio structures.[3] The control of ALD growth

Published on the Web 02/27/2009 www.pubs.acs.org/acr
10.1021/ar800105q CCC: $71.50

is usually ~1 Å per reaction cycle. The resulting ALD films have been shown to be continuous and pinhole-free.[4] ALD techniques have developed in response to the needs for semiconductor device miniaturization and conformal coating on high aspect ratio structures.

Because of the binary nature of the ALD reaction sequence, most ALD materials are binary inorganic compounds. Several reviews have detailed the wide variety of inorganic materials that have been grown using ALD techniques.[5,6] The most common ALD materials are metal oxides and metal nitrides. For example, Al_2O_3 ALD is a model metal oxide that is usually performed using $Al(CH_3)_3$ and H_2O as the two reactants.[7,8] TiN ALD is a well-studied metal nitride that is performed using $TiCl_4$ and NH_3 as the two reactants.[9]

Molecular layer deposition (MLD) is related to ALD and is also based on sequential, self-limiting surface reactions.[10,11] However, in the case of MLD, a "molecular" fragment is deposited during the surface reactions, as shown in Figure 1.[10] This molecular fragment is organic and may also contain inorganic constituents. The deposition of organic polymer MLD films was first achieved using stepwise condensation reactions by several groups in Japan.[11–15] MLD growth with bifunctional reactants has been demonstrated for organic polymers, such as polyamide,[10,14] polyimide,[11,16–18] polyimide–polyamide,[19] polyurea,[20] and polyurethane.[21]

MLD growth methods have also been known as alternating or epitaxial vapor deposition polymerization[14,22] and layer-by-layer[20] growth. The MLD method followed the development of the gas-phase polymer-growth technique known as vapor deposition polymerization (VDP).[22] VDP has been defined for many different stepwise condensation polymers, such as polyimides,[23,24] polyamides,[25,26] and polyureas.[27] The VDP method has been summarized in a previous review.[22]

This paper will discuss the surface chemistry for MLD of polymers. First, the surface chemistry for depositing organic polymers will be examined based on two-step AB reaction cycles with homo-bifunctional reactants. Second, the surface chemistry for hybrid organic–inorganic polymers will be explored based on two-step AB reaction cycles with homo-bifunctional or homo-multifunctional reactants. Subsequently, alternative surface chemical strategies will be examined based on two-step AB reaction cycles with hetero-bifunctional precursors, ring-opening reactions, protected groups, and surface activation. The paper will conclude by discussing three-step ABC reaction cycles with various reactants.

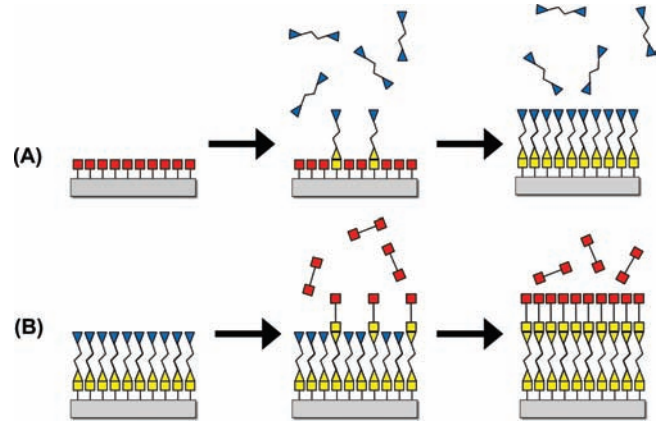

FIGURE 1. Schematic of the MLD method based on sequential, self-limiting surface reactions.

2. Surface Chemistry for MLD of Organic Polymers Based on Two-Step AB Cycles with Homo-bifunctional Reactants

The first studies of MLD of organic polymers focused on polyimides[11] and polyamides.[14] The surface chemistry used homo-bifunctional reactants from stepwise condensation polymerization reactions. The homo-bifunctional reactants were molecules such as XRX and YR'Y. "X" and "Y" are chemical functional groups, and R and R' are organic fragments. A generic two-step AB cycle with two homo-bifunctional reactants is

$$\text{(A)}\quad SR'Y^* + XRX \rightarrow SR'{-}RX^* + XY \qquad (1)$$

$$\text{(B)}\quad SRX^* + YR'Y \rightarrow SR{-}R'Y^* + XY \qquad (2)$$

where the asterisks indicate the surface species. The underlying substrate and deposited film is represented by "S". In the A reaction, the X chemical functionality reacts with SR'Y* species to form SR'–RX* species. In the B reaction, the Y chemical functionality reacts with SRX* species to form SR–R'Y* species.

Surface chemistry studies for MLD of organic polymers based on homo-bifunctional reactants have explored two polyamides: nylon 66[10] and poly(*p*-phenylene terephthalamide) (PPTA).[28] The reactants for nylon 66 MLD are adipoyl chloride ($ClOC{-}(CH_2)_4{-}COCl$) (AC) and 1,6-hexanediamine ($H_2N{-}(CH_2)_6{-}NH_2$) (HD).[10] The acyl chloride and amine functional groups react to form an amide linkage. The surface reactions for nylon 66 are[10]

$$\text{(A)}\quad SNH_2^* + ClCO(CH_2)_4COCl \rightarrow SNH{-}CO(CH_2)_4COCl^* + HCl \qquad (3)$$

(B) $SNHCO(CH_2)_4COCl^* + H_2N(CH_2)_6NH_2 \rightarrow SNHCO(CH_2)_4CO{-}NH(CH_2)_6NH_2^* + HCl$ (4)

When AC is exposed in the "A" reaction, the AC reacts with the amine species and adds $-CO(CH_2)_4COCl^*$ to the surface. When HD is exposed in the "B" reaction, the HD reacts with the acyl chloride species and adds $-NH(CH_2)_6NH_2^*$ to the surface. Alternating exposures of AC and HD in an ABAB... sequence lead to nylon 66 MLD.[10]

The film growth was monitored after sequential exposures of AC and HD for nylon 66 MLD using *in situ* Fourier transform infrared (FTIR) vibrational spectroscopy. Figure 2 shows the vibrational spectra for a nylon 66 MLD film grown on a SiO_2 powder sample versus the number of AB cycles.[10] The absorbances of the N–H and C–H stretching vibrations and the amide I and amide II vibrations grow progressively with number of AB cycles. The integrated absorbance of the amide I and amide II vibrations displayed in Figure 3 illustrates the linear growth of the nylon 66 MLD film versus the number of AB cycles.[10] The integrated absorbance of the C–H stretching vibrations was used to obtain a growth rate for nylon 66 MLD film on flat KBr substrates. These experiments yielded a nylon 66 MLD growth rate of ~19 Å per AB cycle.[10]

The surface chemistry of PPTA MLD has also been examined using terephthaloyl chloride ($ClCOC_6H_4COCl$) (TC) and *p*-phenylenediamine ($NH_2C_6H_4NH_2$) (PD) as the reactants.[28] The acyl chloride and amine functional groups again react to form an amide linkage. Sequential exposures of TC and PD for PPTA MLD were used to deposit this polyamide film. The surface reactions for PPTA MLD are[28]

(A) $SNH_2^* + ClCOC_6H_4COCl \rightarrow SNH{-}COC_6H_4COCl^* + HCl$ (5)

(B) $SNHCO(CH_2)_4COCl^* + H_2NC_6H_4NH_2 \rightarrow SNHCOC_6H_4CO{-}NH(CH_2)_6NH_2^* + HCl$ (6)

A schematic of the surface chemistry during PPTA MLD is shown in Figure 4.[28]

Figure 5 displays the surface chemistry during PPTA MLD on a SiO_2 powder substrate at 145 °C.[28] Figure 5 shows the absolute FTIR spectra of (a) the initial hydroxylated SiO_2 particle substrate, (b) after an aminopropyltrimethyoxysilane (APMS) exposure to deposit amino groups on the surface, (c) after a TC exposure, (d) after a PD exposure, and (e) after another TC exposure.[28] The APMS exposure in Figure 5b reduces the absorbance from isolated O–H stretch vibration on the SiO_2 substrate and produces new absorption peaks from symmetric and asymmetric C–H stretching vibrations. These vibrational features are consistent with APMS reacting with hydroxyl groups on the surface and depositing $-CH_2-$ and $-NH_2$ species.

Terephthaloyl chloride is then exposed to the surface after APMS functionalization. After the TC reaction goes to completion, the signature peak of the acyl chloride surface species in Figure 5c is the absorption from the chlorinated C=O stretching vibrations at 1788 cm^{-1}. Figure 5c also reveals the appearance of the amide I and amide II absorption peaks after the TC exposure. After PD is exposed to the surface following the TC exposure, the absorbance from N–H stretching vibrations grows in the spectra. The loss of absorption from the chlorinated carbonyl stretching vibrations is also clearly monitored at 1788 cm^{-1}. Figure 5d also shows that the PD

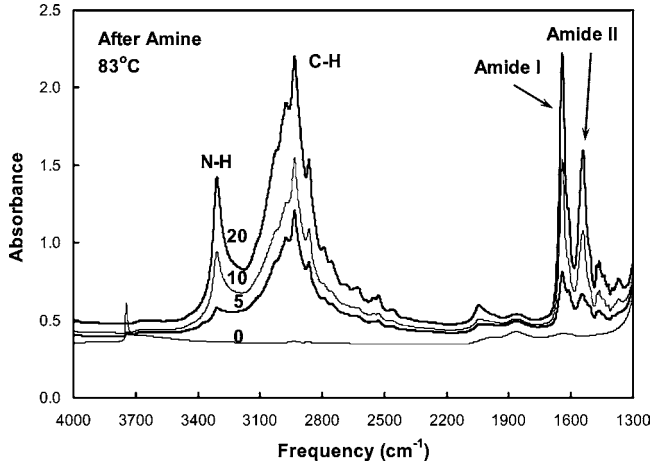

FIGURE 2. FTIR spectra showing an initial hydroxylated SiO_2 surface and during the 5th, 10th, and 20th AB cycles for nylon 66 MLD at 83 °C after HD exposures.

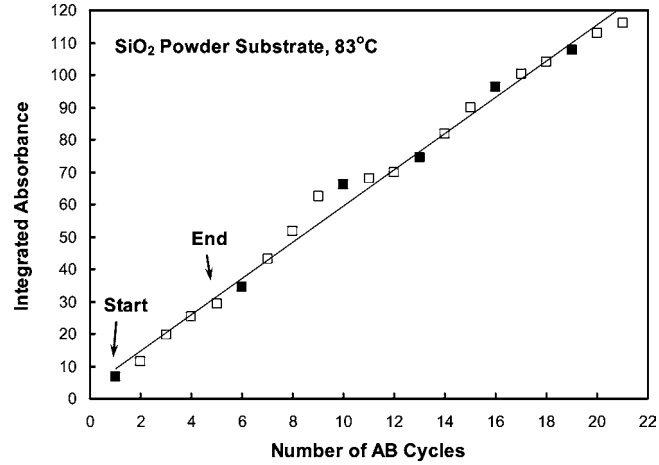

FIGURE 3. Integrated absorbance of amide I and amide II vibrations versus the number of AB cycles for nylon 66 MLD at 83 °C. Solid squares display the first AB cycle recorded during 6 consecutive days of experiments.

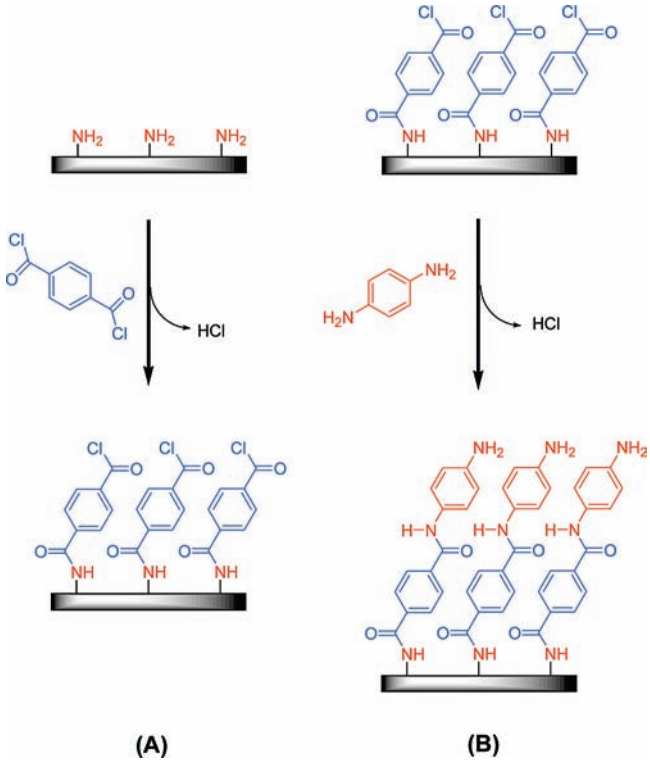

FIGURE 4. Illustration of surface chemistry for PPTA MLD using TC and PD as reactants.

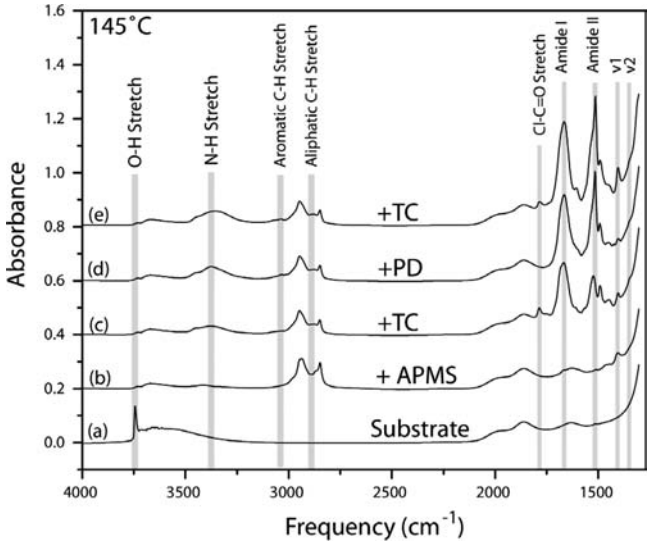

FIGURE 5. FTIR spectra during PPTA MLD at 145 °C showing (a) initial hydroxylated SiO_2 surface, (b) after APMS exposure, (c) after TC exposure, (d) after subsequent PD exposure, and (e) after another TC exposure.

exposures lead to a further increase in absorption from amide I and amide II vibrations. The subsequent TC exposure in Figure 5e again produces absorption from the chlorinated C═O stretching vibrations.

The integrated absorbance of the N–H stretching vibrations and the chlorinated carbonyl stretching vibrations were monitored versus TC and PD exposures to determine if the

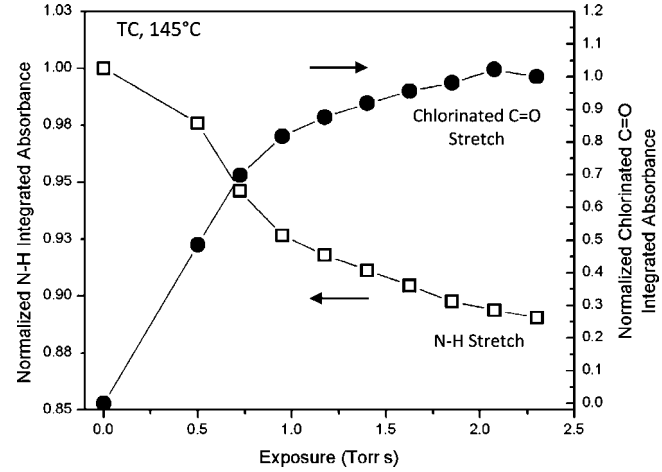

FIGURE 6. Chlorinated carbonyl stretching vibrations and N–H stretching vibrations versus TC exposure for PPTA MLD at 145 °C.

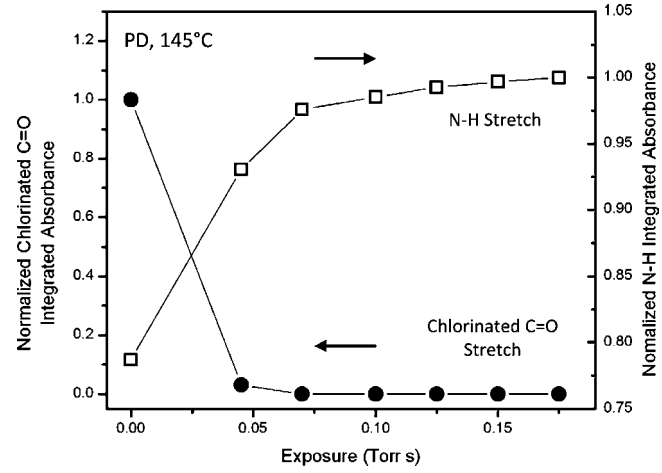

FIGURE 7. Chlorinated carbonyl stretching vibrations and N–H stretching vibrations versus PD exposure for PPTA MLD at 145 °C.

surface reactions were self-limiting. Figure 6 shows the integrated absorbances during TC exposure on the amine surface.[28] The integrated absorbance for the chlorinated carbonyl stretching vibrations reaches a limit at larger TC exposures. In addition, the integrated absorbance of the N–H stretching vibrations is lost concurrently with the gain in the integrated absorbance for the chlorinated carbonyl stretching vibrations. This behavior indicates a self-limiting surface reaction.

Figure 7 shows the integrated absorbances during PD exposure to an acyl chloride surface.[28] The integrated absorbance for the N–H stretching vibrations reaches a limit at larger PD exposures. In addition, the integrated absorbance of the chlorinated carbonyl stretching vibrations is lost concurrently with the gain in the integrated absorbance for the N–H stretching vibrations. This behavior also is consistent with a self-limiting surface reaction.

Polyimide MLD using pyromellitic dianhydride (PMDA) and diamines has also been examined by surface science

techniques.[16,17,29] Electron energy loss investigations monitored the reaction between PMDA and 1,4-phenylene diamine (PDA) and observed the initial formation of amic acid.[16] The amic acid converted to the polyimide with the loss of H_2O. Reflection−absorption infrared spectroscopy was also employed to monitor the growth of polyimide using PMDA and 4,4-oxidianiline (ODA) reactants.[17] Recent studies of polyimide MLD growth have also observed temperature-dependent linear growth rates for polyimide MLD.[18] A growth rate of ~5 Å per AB cycle was measured for polyimide MLD with PMDA and ODA at 160 °C.[18]

MLD reactions with homo-bifunctional reactants can experience difficulties because both functional groups can react with chemical groups on the surface.[10,28] These "double" reactions subtract active sites from the polymer surface and prevent the propagation of the polymer chain growth. Consequently, the "double" reactions progressively poison the thin-film growth. These double reactions can limit the polymer thickness deposited during one AB cycle and lead to irreproducible MLD growth rates.[10,28]

3. Surface Chemistry for MLD of Hybrid Organic−Inorganic Polymers Based on Two-Step AB Cycles with Homo-bifunctional or Homo-multifunctional Reactants

The MLD of hybrid organic−inorganic polymers can be accomplished using an inorganic reactant together with an organic reactant.[30,31] This extension is achieved by combining an inorganic reactant used in a typical ALD process with an organic reactant used in a MLD process. For example, $Al(CH_3)_3$, trimethylaluminum (TMA), is a common metal alkyl reactant used for Al_2O_3 ALD.[7,8] TMA reacts readily with oxygen-containing species. A diol, such as ethylene glycol ($HO(CH_2)_2OH$) (EG), is a homo-bifunctional reactant that could be used together with a carboxylic acid or acyl chloride to deposit a polyester in a MLD process. TMA and EG can be used together in a sequential, stepwise process to deposit a hybrid organic−inorganic polymer.

The general two-step reaction between metal alkyls and diols can be written as[30]

$$\text{(A)}\quad \text{SR'OH}^* + \text{MR}_x \rightarrow \text{SR'O}-\text{MR}_{x-1}{}^* + \text{RH} \qquad (7)$$

$$\text{(B)}\quad \text{SMR}^* + \text{HOR'OH} \rightarrow \text{SM}-\text{OR'OH}^* + \text{RH} \qquad (8)$$

In the A reaction, the reaction reaches completion when all of the SR'OH* species have reacted to produce $SR'O-MR_{x-1}{}^*$ species. In the B reaction, the reaction progresses until all of the SMR* species have completely reacted to produce SM−OR'OH* species. The sequential reactions of TMA and EG yield a polymeric film known as an alucone.[32] A schematic illustrating the growth of this alucone polymer is shown in Figure 8.[30]

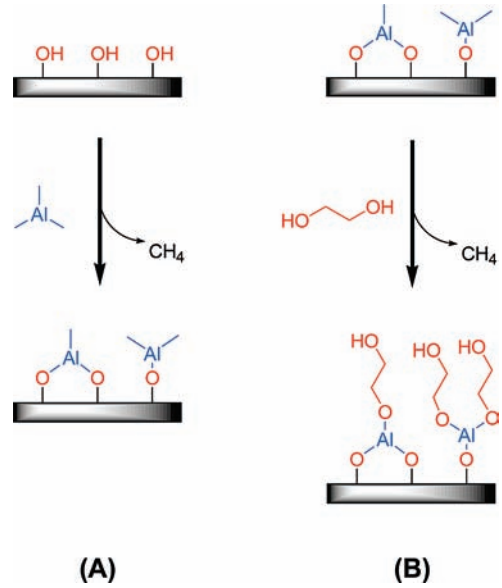

FIGURE 8. Illustration of surface chemistry for poly(aluminum ethylene glycol) alucone MLD using TMA and EG as reactants.

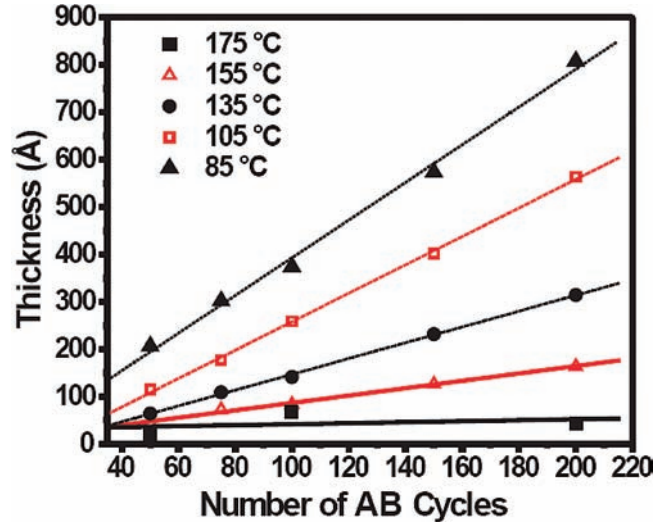

FIGURE 9. Alucone film thickness measured using XRR versus the number of AB cycles using TMA and EG for various deposition temperatures.

Alucone MLD using TMA and EG is very efficient.[30] X-ray reflectivity (XRR) results displayed in Figure 9 reveal that the MLD growth rate is linear versus the number of AB cycles. [30] A summary of the growth rates and film densities versus substrate temperature is summarized in Figure 10. The alucone MLD growth rates decrease from 4.0 Å per AB cycle at 85 °C to 0.4 Å per AB cycle at 175 °C. The density of these alucone films is independent of the deposition temperature and constant at ~1.5 g/cm^3.[30] This alucone film density is much less

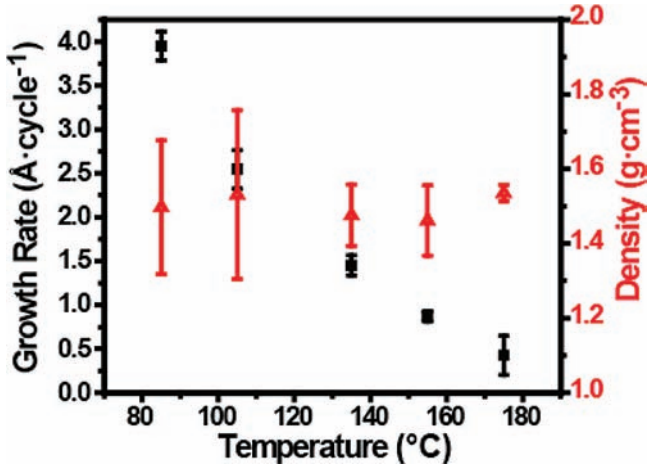

FIGURE 10. Growth per cycle and film density for alucone MLD using TMA and EG for various deposition temperatures.

than the density of ~3.0 g/cm^3 for an Al_2O_3 ALD film grown at 177 °C.[33]

Other organometallic precursors can be employed for the growth of many hybrid organic−inorganic polymers. For example, zinc alkyls, such as $Zn(CH_2CH_3)_2$, diethyl zinc (DEZ), are homo-bifunctional precursors that can react with diols, such as EG, in a similar MLD process.[34] Other metal alkyls and metal halides that can easily react with oxygen are candidates for the MLD of hybrid organic−inorganic polymers. Additional homo-bifunctional organic reactants can expand the generality of these reactions. For example, the homo-bifunctional organic reactant could be a diamine, $H_2N-R-NH_2$, or a dithiol, HS−R−SH, that would form metal nitrides or metal sulfides with various organic constituents.

4. Alternative Surface Chemical Strategies for MLD of Organic and Hybrid Organic−Inorganic Polymers Based on Two-Step AB Cycles

4.1. AB Cycles with Hetero-bifunctional Reactants. MLD reactions can use hetero-bifunctional reactants to avoid double reactions that can decrease the number of active surface species and reduce the MLD growth rate.[28] Hetero-bifunctional reactants have two different chemical functional groups. One of the chemical functional groups can react with the surface species. In contrast, the second chemical functional group does not react or reacts much less preferentially with the surface species. The hetero-bifunctional precursors can minimize double reactions and polymer chain termination.

A general two-step AB cycle using hetero-bifunctional reactants is

$$\text{(A)}\quad SR'Z^* + WRX \rightarrow SR'-RX^* + ZW \qquad (9)$$

$$\text{(B)}\quad SRX^* + YR'Z \rightarrow SR-R'Z^* + XY \qquad (10)$$

In the A reaction, the W chemical functionality on WRX reacts with the SR′Z* species to deposit SR′−RX* species. In the B reaction, the Y chemical functionality on YR′Z reacts with the SRX* species to deposit SR−R′Z* species. There are a variety of examples of hetero-bifunctional reactants that display two separate chemical functionalities on the same molecule.

One class of hetero-bifunctional reactants includes hydroxyl compounds having vinyl functionality, e.g., $HO-RCH=CH_2$. The hydroxyl end of these precursors can react with a carboxylic acid or silicon chloride group to form an ester or silicon−oxygen bond and introduce the vinyl functionality onto the polymer chain. Another type of hetero-bifunctional reactant includes the aminoalcohol compounds, e.g., $H_2N-R-OH$. Either the amino group or the hydroxyl group can react preferentially with surface species. The amino group can react preferentially with a carboxylic acid or an isocyanate group to form an amide or urethane linkage and add hydroxyl functionality on the polymer chain. Alternatively, the hydroxyl group can react preferentially with a silicon chloride group to form a silicon−oxygen bond and introduce an amino group.

4.2. AB Cycles with Ring-Opening Reactions. MLD reactants can also avoid double reactions by containing a concealed functionality that only expresses itself upon reaction. Many ring-opening reactions yield new hydroxyl, amine, or carboxylic acid groups upon reaction. For example, a cyclic azasilane (AZ), such as 2,2-dimethoxy-1,6-diaza-2-silacyclooctane, can react with a surface hydroxyl to create a silicon−oxygen bond.[28,35] The cyclic azasilane also unfolds, leaving amine species that are not expected to be reactive with surface hydroxyl groups. A cyclic carbonate, such as ethylene carbonate (EC), can then react with a surface amine to form a urethane linkage.[28] The ethylene carbonate also unfolds and produces hydroxyl species that are not expected to be reactive with surface amine groups. A schematic showing these two ring-opening reactions is displayed in Figure 11.

These MLD reactions can be followed using *in situ* FTIR vibrational spectroscopy.[28] FTIR spectra recorded at 120 °C are displayed in Figure 12. The spectrum of the starting SiO_2 powder substrate in Figure 12a shows a sharp absorption peak for O−H stretching vibrations from isolated hydroxyl groups on the surface. Lower frequency absorption features from the bulk SiO_2 powder also appear at <1400 cm^{-1}. After the reaction of the AZ, the absorption peak associated with the isolated hydroxyl groups disappears and the spectrum in Figure 12b displays absorbances from C−H and N−H stretching

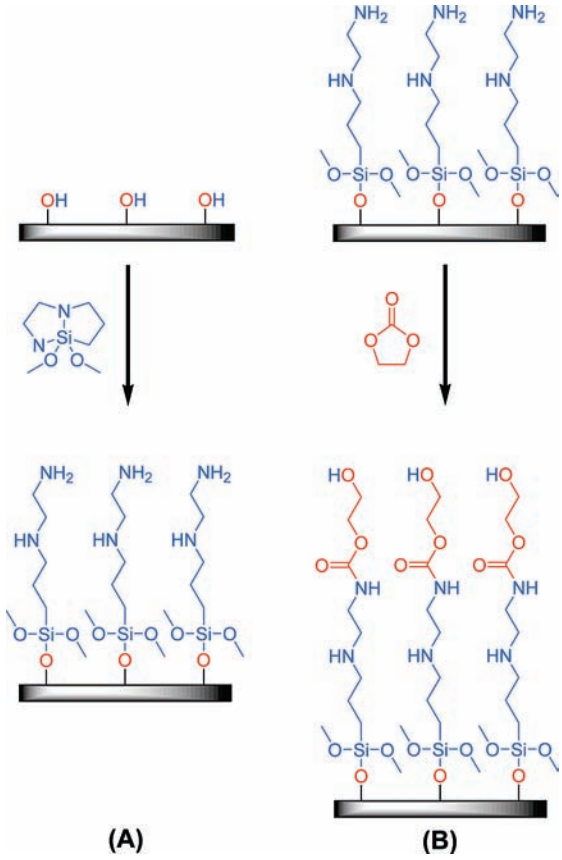

FIGURE 11. Illustration of surface chemistry involving two ring-opening reactions with AZ and EC as reactants.

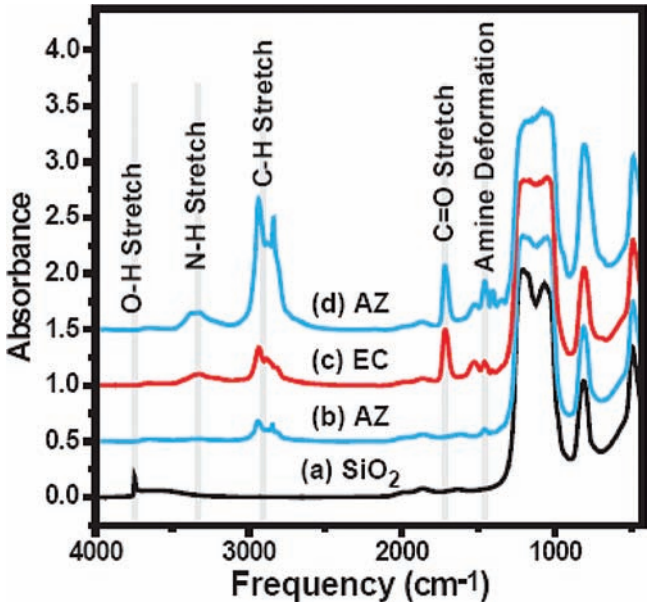

FIGURE 12. FTIR spectra during two ring-opening reactions with AZ and EC at 120 °C showing (a) initial hydroxylated SiO_2 surface, (b) after AZ exposure, (c) after EC exposure, and (d) after subsequent AZ exposure.

vibrations and amine deformation modes. These absorption features are expected after the reaction of AZ, as illustrated in Figure 11.

The spectrum after the subsequent reaction of EC shown in Figure 12c induces increases in the absorbance for the C−H stretching vibrations and intensifies the absorbance of the N−H stretching vibrations and amine deformation modes. In addition, a strong absorption peak is observed from C═O stretching vibrations. These infrared features are expected after the reaction of EC, as shown in Figure 11. The spectrum shown in Figure 12d after the subsequent AZ exposure increases the absorbance for the C−H and N−H stretching vibrations and the amine deformation modes.

4.3. AB Cycles Using Reactants with Protected Groups. Reactants that contain two different reactive groups, where one reactive group is protected from reaction, also avoid the use of homo-bifunctional reactants. For these precursors, one functional group is not available for reaction until removal of the protecting group. The protective group can be removed by a chemical reaction. Alternatively, the protective group can be removed by radiating the group with light to induce a photochemical reaction.

An illustration of this class of MLD reaction with protected groups is shown in Figure 13. This reaction sequence has not yet been confirmed by experiments. In the first step, a hydroxylated surface is exposed to 3-(1,3-dimethylbutylidene) aminopropyltriethoxysilane (DAPS). The DAPS binds to the surface through a siloxane linkage. A protecting imine group hides the $-NH_2$ functionality. Exposure to water then reacts with the imine moiety and releases 4-methyl-2-pentanone. This reaction leaves a surface terminated with primary amine groups.

The surface can then be exposed to an acyl chloride, such as 1-(*o*-nitrobenzyl)-3-oxyheptanoyl chloride (NOC). This acyl chloride precursor adds to the surface via an amide linkage and yields a nitrobenzyl-protected surface. The nitrobenzyl-protection group hides an underlying hydroxyl group. The hydroxyl group is then deprotected by exposure to ultraviolet (UV) light.[36] The UV light removes the nitrobenzyl group and unmasks the hidden hydroxyl chemical functionality. The reaction sequence can then proceed with another exposure to DAPS.

4.4. AB Cycles with Surface Activation. Homo-bifunctional reactants can also be avoided using reactions where surface activation is used to create a chemical functional group. In this class of surface reactions, one functional group on a hetero-bifunctional precursor reacts with an active surface species. Additional chemistry is then performed to transform the second functional group to a more active chemical functional group. One notable functional group that can be

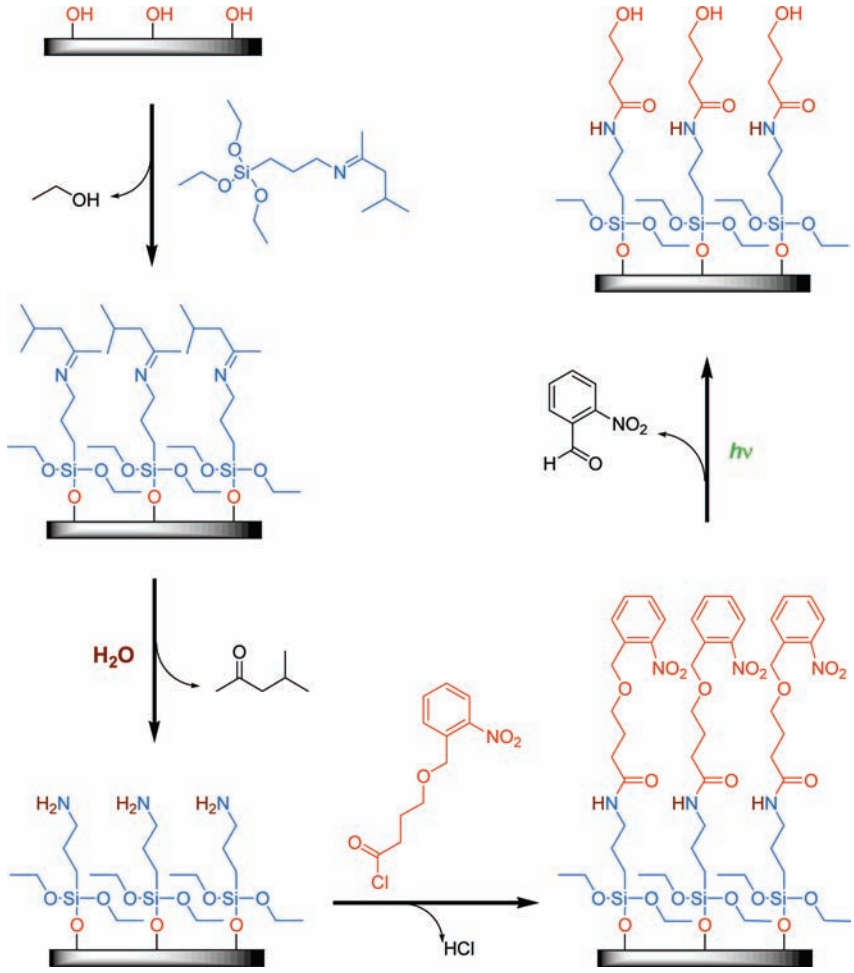

FIGURE 13. Illustration of the surface chemistry involving protected groups. The initial hydroxylated surface is first exposed to DAPS. H_2O then removes the protecting group and exposes amine functionality. NOC reacts with amine functionality. The hydroxyl group is then deprotected using UV light exposure to complete the reaction cycle.

activated is a vinyl group. Vinyl groups can react with ozone or peroxides to form carboxylic acids or aldehydes.

An example of an organic–inorganic polymer formed using surface activation uses trimethylaluminum (TMA) and 3-buten-1-ol (BTO) as the precursors as shown in Figure 14. This reaction sequence has been confirmed by preliminary *in situ* FTIR experiments.[28] The reaction begins with a hydroxylated surface. Subsequently, a layer of $AlCH_3^*$ species are deposited by exposure to TMA. BTO is then exposed to the surface. The hydroxylated end of the BTO precursor reacts with the aluminum atom of the $AlCH_3^*$ surface species to create an Al–O bond and displaces methane. When this reaction occurs, the vinyl group on the other end of the BTO precursor is orientated away from the surface. The vinyl group is then activated by exposure to ozone to form a carboxylic acid. The hydroxyl group of the carboxylic acid can then react with TMA to repeat the reaction cycle.[28]

The surface activation mechanism technique has also been demonstrated by recent work using the sequential growth of alkylsilozane self-assembled monolayers with vinyl termination.[37] After conversion of the vinyl functionality to carboxylic acid functionality using ozone, the film was converted to titanium hydroxide using $TiCl_4$ and H_2O. The alkylsilozane self-assembled monolayer was then deposited again on the titanium hydroxide surface. This method has been shown to deposit organic–inorganic hybrid superlattices with monolayer precision that display thermal and mechanical stability.[37]

5. Surface Chemistry for Polymer MLD Based on Three-Step ABC Cycles

The MLD of organic and hybrid organic–inorganic polymers can also be accomplished using a three-step ABC reaction sequence. Three-step ABC reactions increase the flexibility of MLD reactions to include various organic compositions. In

addition, three-step ABC reactions enlarge the number of different combinations of possible hetero-bifunctional reactants that can be used to define the MLD process.

Many of the most reactive precursors, such as TMA and DEZ, are homo-multifunctional reactants. These precursors can react to form a chemical bond or coordinate through Lewis acid/base interactions. The homo-multifunctional precursors are susceptible to double reactions in a two-step AB cycle. However, these reactants can work effectively in a three-step ABC cycle with two other hetero-bifunctional reactants. The three-step ABC cycle helps to minimize the poisoning effect of the double reactions.

There are many possible three-step ABC cycles involving three hetero-bifunctional reactants. Assuming three hetero-bifunctional precursors: TRV, WR′X, and YR″Z, the three-step ABC cycle is

$$\text{(A)}\quad \text{SR''Z}^* + \text{TRV} \rightarrow \text{SR''–RV}^* + \text{ZT} \qquad (11)$$

$$\text{(B)}\quad \text{SRV}^* + \text{WR'X} \rightarrow \text{SR–R'X}^* + \text{VW} \qquad (12)$$

$$\text{(C)}\quad \text{SR'X}^* + \text{YR''Z} \rightarrow \text{SR'–R''Z}^* + \text{XY} \qquad (13)$$

There are also many three-step ABC cycles with one homo-multifunctional reactant and two hetero-bifunctional reactants. A variety of combinations also exists for three-step ABC cycles using homo-multifunctional reactants, hetero-bifunctional reactants, and the other ring-opening reactions, surface activation and protective group strategies.

An example of a three-step ABC reaction is (A) $Al(CH_3)_3$, trimethylaluminum (TMA), (B) $HOCH_2CH_2NH_2$, ethanolamine (EA),

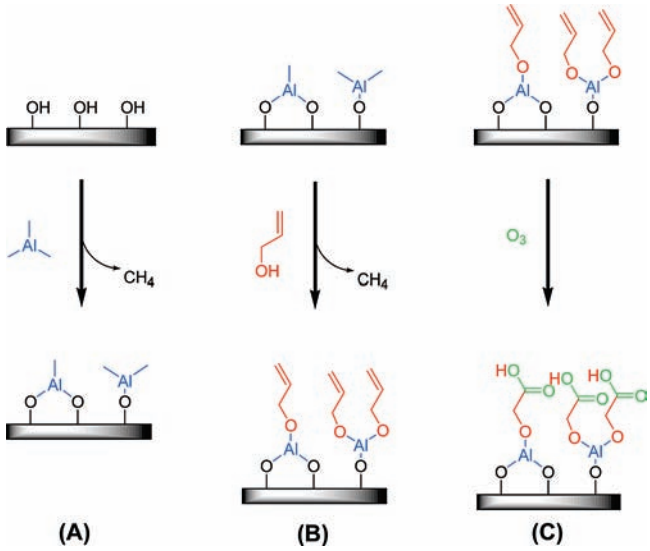

FIGURE 14. Illustration of the surface chemistry involving surface activation. TMA first reacts with the hydroxylated surface. The hydroxyl end of BTO then reacts and yields the surface terminated by vinyl groups. Vinyl groups are then exposed to ozone to form carboxylic acid groups.

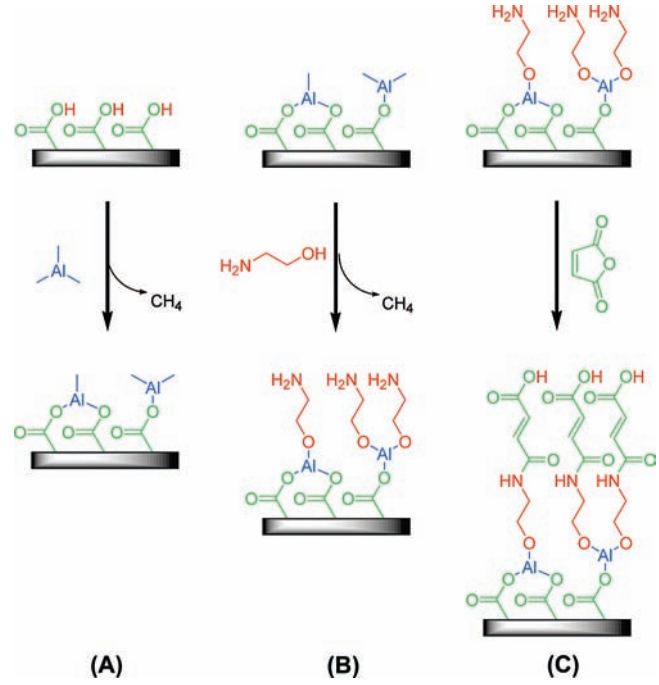

FIGURE 15. Illustration of the surface chemistry for the three-step ABC cycle with TMA, EA, and MA as reactants.

and (C) $C_4H_2O_3$, maleic anhydride (MA).[38] TMA is a homo-trifunctional reactant; EA is a hetero-bifunctional reactant; and MA is a ring-opening reactant. This MLD reaction is shown schematically in Figure 15. In this reaction sequence, TMA reacts with hydroxyl groups in the A reaction to form $AlCH_3^*$ surface species. EA then reacts with $AlCH_3^*$ surface groups to form $AlOCH_2CH_2NH_2^*$ surface species in the B reaction. MA then reacts with the NH_2^* surface groups to reform hydroxyl groups on the surface in the C reaction. The ABC... sequence is then repeated by exposure to TMA, EA, and MA.

The surface reactions during the ABC sequence can be monitored using *in situ* FTIR vibrational spectroscopy. FTIR difference spectra recorded at 150 °C are shown in Figure 16.[38] The TMA–MA difference spectra in Figure 16a shows the expected increase in absorbance from the C–H stretching vibrations and methyl deformation modes from the $AlCH_3^*$ surface species. There is also an increase in absorbance from the carbonyl modes from the new COO–Al surface species and the loss of absorbance from O–H stretching vibrations after the TMA reaction. The EA–TMA difference spectrum in Figure 16b observes the increase in absorbance from the N–H, C–H, and C–O stretching vibrations and the loss of absorbance from the methyl deformation modes after the EA reaction. The MA–EA difference spectrum in Figure 16c displays the increase in absorbance from the O–H stretching vibrations, the carbonyl modes from the carboxylic acid groups, and amide I and amide II vibrations after the MA reaction.

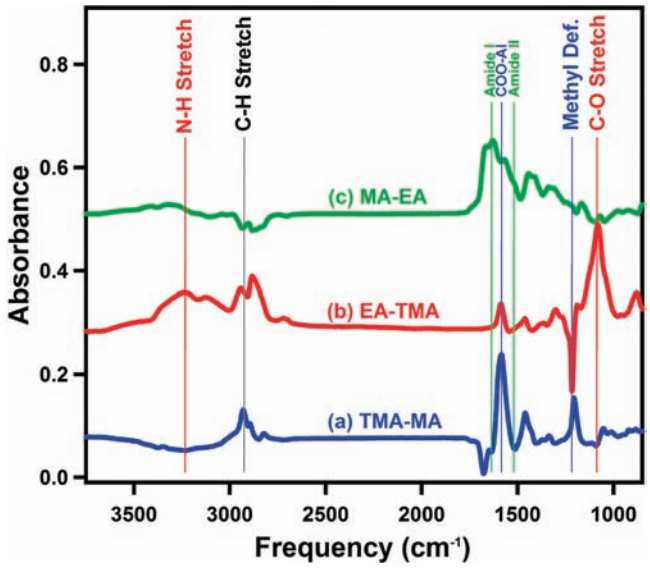

FIGURE 16. FTIR difference spectra during the three-step ABC reaction sequence with TMA, EA, and MA at 150 °C: (a) after TMA reaction, (b) after EA reaction, and (c) after MA reaction.

The ABC reaction sequence with TMA, EA, and MA produces excellent film growth versus the number of ABC cycles. The C–H and N–H stretching vibrations and the amide I and amide II vibrations are observed to grow linearly versus the number of ABC cycles.[38] Recent XRR studies have shown that the growth rate of the ABC alucone film decreases with temperature and varies from 24 Å per ABC cycle at 90 °C to 8 Å per ABC cycle at 150 °C.[38]

6. Challenges and Future Prospects

Organic chemistry and polymer processing have been extensively developed using solution-phase techniques. Although synthesis in liquids is tremendously important, the ability to deposit ultra-thin and conformal polymer films in condensed phases is difficult. Much higher degrees of control can be realized using gas-phase methods, as demonstrated by ALD techniques for the growth of inorganic materials. The MLD of polymers has proven that the strategy of using sequential, self-limiting reactions can be extended to polymeric materials. The translation of additional organic chemistry into the gas phase will be important for the continued development of gas-phase polymer-growth techniques.

One challenge of performing organic chemistry in the gas phase is finding organic reactants that have sufficient vapor pressure. If the reactants have low vapor pressure, then reaction rates can be low and the reactants may require very long purge times. Increasing the vapor pressure is also not easily overcome by increasing the precursor temperature because of the thermal fragility of organic reactants. Another challenge of performing organic chemistry in the gas phase is understanding the effect of the solution phase on the reaction. Many organic reactions are catalyzed by acid or base or influenced by solvation effects that are absent in the gas phase. Similar condensed-phase environments that are necessary for many organic reactions may be difficult to reconstruct in the gas phase.

Another challenge for polymer MLD is the porous nature of the polymer. This porosity can lead to the diffusion of gas-phase reactants into the polymer. Earlier studies of ALD on polymers showed that ALD can nucleate and grow on a variety of polymers because the reactants can diffuse into the polymer and stay absorbed after the reactant exposure.[39–41] These absorbed reactants can then react with the subsequent reactant and lead to film growth. Similar pathways also exist during sequential surface reactions on polymers. The reactants can either react directly with surface species on the growing polymer or diffuse into the polymer. MLD growth may then occur by both surface and bulk diffusion mechanisms. The diffusion mechanisms should enhance the MLD growth rates by adding a contribution similar to CVD. However, the MLD growth may still be self-limiting if the reactant absorption is predominantly in the near surface region of the polymer.

Despite the challenges for polymer MLD, the prospects for advancement of polymer MLD are very encouraging. Many new surface chemistry strategies are being developed that will increase the number of materials that can be deposited using MLD. These new MLD methods can also be coupled with existing ALD techniques to fabricate a variety of composite materials. The behavior of these MLD and composite MLD/ALD films will be interesting because their mechanical properties can vary from flexible soft polymers to brittle hard ceramics. The sequential nature of MLD growth may also lead to polymer chain alignment and significant anisotropies. The MLD of polymers should become an important technique for thin-film growth and nanofabrication. Many opportunities are on the horizon, and surface chemistry should continue to play a vital role.

We thank the previous co-workers in the George group, Yijun Du and Nicole M. Adamcyzk, who contributed to our understanding of molecular layer deposition of polymers. This work was funded by the National Science Foundation under Grant CHE-0715552. Additional support was provided by the Air Force Office of Scientific Research.

BIOGRAPHICAL INFORMATION

Steven M. George (B.S. degree in chemistry in 1977 from Yale University and Ph.D. degree in chemistry in 1983 from the University

of California at Berkeley) leads a group at the University of Colorado at Boulder that is focusing on surface chemistry, thin film growth, and nanostructure engineering.

Byunghoon Yoon (B.S. degree in chemistry in 1996 and M.S. degree in chemistry in 1998 both from Kyung Hee University and Ph.D. degree in chemistry in 2006 from the University of Idaho) is studying the surface chemistry of molecular layer deposition as a postdoctoral research associate at the University of Colorado at Boulder.

Arrelaine A. Dameron (B.S. degree in creative studies in 2001 from the University of California at Santa Barbara and Ph.D. degree in chemistry in 2006 from Pennsylvania State University) was a postdoctoral research associate at the University of Colorado at Boulder. She is currently working at the National Renewable Energy Laboratory in Golden, CO.

FOOTNOTES

*To whom correspondence should be addressed. Fax: 303-492-5894. E-mail: steven.george@colorado.edu.

§Current address: National Renewable Energy Laboratory, 1617 Cole Blvd., Golden, CO 80401.

REFERENCES

1 George, S. M.; Ott, A. W.; Klaus, J. W. Surface chemistry for atomic layer growth. *J. Phys. Chem.* **1996**, *100*, 13121–13131.

2 Suntola, T. Atomic layer epitaxy. *Thin Solid Films* **1992**, *216*, 84–89.

3 Ritala, M.; Leskela, M.; Dekker, J. P.; Mutsaers, C.; Soininen, P. J.; Skarp, J. Perfectly conformal TiN and Al_2O_3 films deposited by atomic layer deposition. *Chem. Vap. Deposition* **1999**, *5*, 7–9.

4 Groner, M. D.; Elam, J. W.; Fabreguette, F. H.; George, S. M. Electrical characterization of thin Al_2O_3 films grown by atomic layer deposition on silicon and various metal substrates. *Thin Solid Films* **2002**, *413*, 186–197.

5 Puurunen, R. L. Surface chemistry of atomic layer deposition: A case study for the trimethylaluminum/water process. *J. Appl. Phys.* **2005**, *97*, 121301.

6 Ritala, M.; Leskela, M. Atomic layer deposition. In *Handbook of Thin Film Materials*; Nalwa, H. S., Ed.; Academic Press: New York, 2001; Vol. 1.

7 Dillon, A. C.; Ott, A. W.; Way, J. D.; George, S. M. Surface chemistry of Al_2O_3 deposition using $Al(CH_3)_3$ and H_2O in a binary reaction sequence. *Surf. Sci.* **1995**, *322*, 230–242.

8 Ott, A. W.; Klaus, J. W.; Johnson, J. M.; George, S. M. Al_2O_3 thin film growth on Si(100) using binary reaction sequence chemistry. *Thin Solid Films* **1997**, *292*, 135–144.

9 Ritala, M.; Leskela, M.; Rauhala, E.; Haussalo, P. Atomic layer epitaxy growth of TiN thin films. *J. Electrochem. Soc.* **1995**, *142*, 2731–2737.

10 Du, Y.; George, S. M. Molecular layer deposition of nylon 66 films examined using in situ FTIR spectroscopy. *J. Phys. Chem. C* **2007**, *111*, 8509–8517.

11 Yoshimura, T.; Tatsuura, S.; Sotoyama, W. Polymer films formed with monolayer growth steps by molecular layer deposition. *Appl. Phys. Lett.* **1991**, *59*, 482–484.

12 Kubono, A.; Yuasa, N.; Shao, H. L.; Umemoto, S.; Okui, N. In situ study on alternating vapor deposition polymerization of alkyl polyamide with normal molecular orientation. *Thin Solid Films* **1996**, *289*, 107–111.

13 Nagai, A.; Shao, H. L.; Umemoto, S.; Kikutani, T.; Okui, N. Quadruple aliphatic polyamide systems prepared by a layer-by-layer alternating vapour deposition method. *High Perform. Polym.* **2001**, *13*, S169–S179.

14 Shao, H. I.; Umemoto, S.; Kikutani, T.; Okui, N. Layer-by-layer polycondensation of nylon 66 by alternating vapour deposition polymerization. *Polymer* **1997**, *38*, 459–462.

15 Yoshimura, T.; Tatsuura, S.; Sotoyama, W.; Matsuura, A.; Hayano, T. Quantum wire and dot formation by chemical vapor deposition and molecular layer deposition of one-dimensional conjugated polymer. *Appl. Phys. Lett.* **1992**, *60*, 268–270.

16 Bitzer, T.; Richardson, N. V. Demonstration of an imide coupling reaction on a Si(100)-2×1 surface by molecular layer deposition. *Appl. Phys. Lett.* **1997**, *71*, 662–664.

17 Haq, S.; Richardson, N. V. Organic beam epitaxy using controlled PMDA–ODA coupling reactions on Cu{110}. *J. Phys. Chem. B* **1999**, *103*, 5256–5265.

18 Putkonen, M.; Harjuoja, J.; Sajavaara, T.; Niinisto, L. Atomic layer deposition of polyimide thin films. *J. Mater. Chem.* **2007**, *17*, 664–669.

19 Miyamae, T.; Tsukagoshi, K.; Matsuoka, O.; Yamamoto, S.; Nozoye, H. Preparation of polyimide–polyamide random copolymer thin film by sequential vapor deposition polymerization. *Jpn. J. Appl. Phys., Part 1* **2002**, *41*, 746–748.

20 Kim, A.; Filler, M. A.; Kim, S.; Bent, S. F. Layer-by-layer growth on Ge(100) via spontaneous urea coupling reactions. *J. Am. Chem. Soc.* **2005**, *127*, 6123–6132.

21 Lee, J. S.; Lee, Y. J.; Tae, E. L.; Park, Y. S.; Yoon, K. B. Synthesis of zeolite as ordered multicrystal arrays. *Science* **2003**, *301*, 818–821.

22 Kubono, A.; Okui, N. Polymer thin films prepared by vapor deposition. *Prog. Polym. Sci.* **1994**, *19*, 389–438.

23 Salem, J. R.; Sequeda, F. O.; Duran, J.; Lee, W. Y.; Yang, R. M. Solventless polyimide films by vapor deposition. *J. Vac. Sci. Technol., A* **1986**, *4*, 369–374.

24 Takahashi, Y.; Iijima, M.; Inagawa, K.; Itoh, A. Synthesis of aromatic polyimide film by vacuum deposition polymerization. *J. Vac. Sci. Technol., A* **1987**, *5*, 2253–2256.

25 Kubono, A.; Okui, N.; Tanaka, K.; Umemoto, S.; Sakai, T. Highly oriented polyamide thin films prepared by vapor deposition polymerization. *Thin Solid Films* **1991**, *199*, 385–393.

26 Takahashi, Y.; Iijima, M.; Oishi, Y.; Kakimoto, M.; Imai, Y. Preparation of ultrathin films of aromatic polyamides and aromatic poly(amide imides) by vapor deposition polymerization. *Macromolecules* **1991**, *24*, 3543–3546.

27 Takahashi, Y.; Iijima, M.; Fukada, E. Pyroelectricity in poled thin films of aromatic polyurea prepared by vapor deposition polymerization. *Jpn. J. Appl. Phys., Part 2* **1989**, *28*, L2245–L2247.

28 Adamczyk, N. M.; Dameron, A. A.; George, S. M. Molecular layer deposition of poly(*p*-phenylene terephthalamide) films using terephthaloyl chloride and *p*-phenylenediamine. *Langmuir* **2008**, *24*, 2081–2089.

29 Frederick, B. G.; Richardson, N. V.; Unertl, W. N.; Elfarrash, A. Reaction of aniline with chemisorbed pyromellitic dianhydride on Cu(110)—A model for controlled organic film growth. *Surf. Interface Anal.* **1993**, *20*, 434–440.

30 Dameron, A. A.; Seghete, D.; Burton, B. B.; Davidson, S. D.; Cavanagh, A. S.; Bertrand, J. A.; George, S. M. Molecular layer deposition of alucone polymer films using trimethylaluminum and ethylene glycol. *Chem. Mater.* **2008**, *20*, 3315–3326.

31 We initially reported our results on alucone MLD at the AVS Topical Conference on Atomic Layer Deposition (ALD2007) in San Diego, CA (Dameron, A. A.; et al. Molecular layer deposition of alucone polymer films using trimethylaluminum and ethylene glycol. AVS Topical Conference on Atomic Layer Deposition (ALD2007), San Diego, CA, June 26, 2007). We learned about a patent application that describes related work during a presentation by O. Nilsen at ALD2007 (Nilsen, O.; Fjellvag, H. Thin films prepared with gas phase deposition technique. Patent Cooperation Treaty, World Intellectual Property Organization, WO 2006/071126 A1, July 6, 2006).

32 McMahon, C. N.; Alemany, L.; Callender, R. L.; Bott, S. G.; Barron, A. R. Reaction of $Al(Bu\text{-}t)_3$ with ethylene glycol: Intermediates to aluminum alkoxide (alucone) preceramic polymers. *Chem. Mater.* **1999**, *11*, 3181–3188.

33 Groner, M. D.; Fabreguette, F. H.; Elam, J. W.; George, S. M. Low temperature Al_2O_3 atomic layer deposition. *Chem. Mater.* **2004**, *16*, 639–645.

34 Yoon, B.; O'Patchen, J. L.; Seghete, D.; Cavanagh, A. S.; George, S. M. Molecular layer deposition of hybrid organic–inorganic polymer films using diethyl zinc and ethylene glycol. *Chem. Vap. Deposition* **2009**, in press.

35 Arkles, B.; Pan, Y.; Larson, G. L.; Berry, D. H. Cyclic azasilanes: Volatile coupling agents for nanotechnology. In *Silanes and Other Coupling Agents*; Mittal, K. L., Ed.; VSP: Utrecht, The Netherlands, 2004; Vol. 3, pp 179–191.

36 Zubkov, T.; Lucassen, A. C. B.; Freeman, D.; Feldman, Y.; Cohen, S. R.; Evmenenko, G.; Dutta, P.; van der Boom, M. E. Photoinduced deprotection and ZnO patterning of hydroxyl-terminated siloxane-based monolayers. *J. Phys. Chem. B* **2005**, *109*, 14144–14153.

37 Lee, B. H.; Ryu, M. K.; Choi, S. Y.; Lee, K. H.; Im, S.; Sung, M. M. Rapid vapor phase fabrication of organic–inorganic hybrid superlattices with monolayer precision. *J. Am. Chem. Soc.* **2007**, *129*, 16034–16041.

38 Yoon, B.; Seghete, D.; George, S. M. Molecular layer deposition of alucone polymer film using a three-step ABC reaction sequence. 2009, unpublished results.

39 Elam, J. W.; Wilson, C. A.; Schuisky, M.; Sechrist, Z. A.; George, S. M. Improved nucleation of TiN atomic layer deposition films on SILK low-k polymer dielectric using an Al_2O_3 atomic layer deposition adhesion layer. *J. Vac. Sci. Technol., B* **2003**, *21*, 1099–1107.

40 Ferguson, J. D.; Weimer, A. W.; George, S. M. Atomic layer deposition of Al_2O_3 films on polyethylene particles. *Chem. Mater.* **2004**, *16*, 5602–5609.

41 Wilson, C. A.; Grubbs, R. K.; George, S. M. Nucleation and growth during Al_2O_3 atomic layer deposition on polymers. *Chem. Mater.* **2005**, *17*, 5625–5634.